https://doi.org/10.5194/gc-2019-16
Preprint. Discussion started: 6 September 2019

Geoscience Communication Discussions
Open Access
EGU

Novel index to comprehensively evaluate air cleanness: the "Clean aIr Index"

Tomohiro O. Sato[1], Takeshi Kuroda[2,1], and Yasuko Kasai[1,3]

[1]National Institute of Information and Communications Technology
[2]Tohoku University
[3]University of Tsukuba

Correspondence: Yasuko Kasai (ykasai@nict.go.jp)

Abstract. Air quality on our planet has been changing in particular since the industrial revolution (1750s) because of anthropogenic emissions. It is becoming increasingly important to visualize air cleanness, since clean air deserves a valuable resource as clean water. We defined a novel concept, namely "Clean aIr Index, CII," to quantify the level of air cleanness in terms of a global standard. The CII is a simple index defined by the normalization of the amount of individual air pollutants. A CII value of 1 indicates completely clean air (no air pollutants), and 0 indicates the presence of air pollutants up to numerical environmental criteria for the normalization. In this time, the air pollutants used in the CII were taken from the Air Quality Guidelines (AQG) set by the World Health Organization (WHO), namely O_3, particulate matters, NO_2 and SO_2. We chose Japan as a study area to evaluate CII because of the following reasons: i) accurate validation data, as the in situ observation sites of the Atmospheric Environmental Regional Observation System (AEROS) provide highly accurate values of air pollutant amounts, ii) obvious numerical criteria, namely the Japanese Environmental Quality Standards given by the Ministry of the Environment (MOE). We quantified air cleanness in terms of the CII for the all 1896 municipalities in Japan, and used Seoul and Beijing to evaluate Japanese air cleanness. The amount of each air pollutant was calculated using a model that combined the Weather Research and Forecasting (WRF) and Community Multiscale Air Quality (CMAQ) models for 1 April 2014 to 31 March 2017. The CII values were validated by comparing the WRF-CMAQ model and AEROS measurements for selected six cities, and an average correlation coefficient of > 0.61 was obtained. The CII value of Tokyo averaged for the study period was 0.75, which was 1.2 and 1.9 times higher than that of Seoul (0.64) and Beijing (0.39), respectively. The extremely clean air, CII > 0.93, occurred around west of the Pacific coast, i.e., Kochi, Mie and Wakayama Prefectures, and southern remote islands of Tokyo during summer with transport of clean air from the ocean. The average CII value for the all Japanese municipalities was 0.78 over the study period. We presented "Top 100 clean air cities" in Japan using the CII. We confirmed that the CII enabled the quantitative evaluation of air cleanness. The CII can be useful value, for example, for encouraging sightseeing and migration, as "tasty air," insurance company business, and city planning. The CII is a simple and fair index that can be applied to all nations.

https://doi.org/10.5194/gc-2019-16
Preprint. Discussion started: 6 September 2019

GEOSCIENCE COMMUNICATION Discussions
Open Access
EGU

1 Introduction

Air is an essential components for all life on our planet. Air quality has been changing since the industrial revolution (1750s). Furthermore, air pollutant emissions are predicted to increase because of the projected increase in the energy demand, e.g., transportation and power generation, especially in East Asia, and the global annual market costs of reduced labor productivity, increased health expenditures, and crop yield losses due to air pollution are predicted to increase global GDP from 0.3 % in 2015 to 1.0 % by 2060 (OECD, 2016). Air quality is also an important issue in city planning (e.g., McCarty and Kaza, 2015). Therefore, a global standard index to quantify air cleanness should be developed, since clean air is as valuable a resource as clean water is. Such an index can be a useful communication tool to allow people to make more informed choices. The index should be upgraded with the scientific data, and be understandable/informative not only for scientific experts but also general citizen.

Several indexes exist for estimating air quality, e.g., Air Quality Index in the United States (US EPA, 2006) and Air Quality Health Index in Canada (Stieb et al., 2008) and Hong Kong (Wong et al., 2013). The purpose of these indexes is to estimate health risks due to air pollution exposure. These indexes were developed based on epidemiological studies and optimized for each country or local area. However, a global standard index for quantifying air cleanness has not been developed.

In this study, we propose a novel concept of index to quantify air cleanness, "Clean aIr Index (CII)." The purpose of CII is to comprehensively evaluate air cleanness by normalizing the amounts of common air pollutants with numerical environmental criteria. In this time, we selected surface O_3, particulate matter (PM), NO_2, and SO_2 from the Air Quality Guidelines (AQG) set by the World Health Organization (WHO)(WHO, 2005). The CII can be used globally and locally by optimizing the numerical criteria. As a first approach, we chose Japan for evaluating the CII because of i) the validation data, as the in situ observation sites of the Atmospheric Environmental Regional Observation System (AEROS) provide highly accurate air pollutant amounts, and ii) the obvious numerical criteria, i.e., the Japanese Environmental Quality Standards given by the Ministry of the Environment (MOE).

In this paper, Sect. 2 introduces the CII. Section 3 describes the model for calculating the CII for all Japanese municipalities, and validates the CII by comparing it with that derived from AEROS measurements. In Sect. 4, air cleanness in each municipality is quantified using the CII.

2 Clean aIr Index

The CII is a simple index defined by the normalization of each air pollutant amount. The definition of CII is given by

$$\mathrm{CII} = f(x,s) = 1 - \frac{1}{\mathrm{N}} \sum_{i}^{\mathrm{N}} \frac{x[i]}{s[i]}, \tag{1}$$

where $x[i]$ is the amount of ith air pollutant, $s[i]$ is the numerical criteria for the normalization of $x[i]$, and N is the number of air pollutants considered in this study. In this equation, a higher CII value indicates cleaner air, with a maximum of 1 indicating the absence of air pollutants. The CII value decreases as the amount of air pollutant increases, with a value of 0 indicating that

https://doi.org/10.5194/gc-2019-16
Preprint. Discussion started: 6 September 2019

GEOSCIENCE COMMUNICATION Discussions
Open Access
EGU

Table 1. Value of numerical criteria (s), O_3, suspended particulate matter (SPM), NO_2, and SO_2 used in this study. We used the criteria of the Japanese Environmental Quality Standards (JEQS) given by the Ministry of the Environment (MOE) of Japan. Average of air pollutant amount calculated by the model for all Japanese municipalities over the study period is shown. Criterion for photochemical oxidants (Ox) in JEQS was used as the s value for O_3, because more than 90–95 % of Ox is composed of O_3.

Air pollutant	Average of model	Numerical criteria (s)	Notes
O_3	31.9 ppb	60 ppb	Threshold of the hourly values
SPM	13.5 μg/m^3	100 μg/m^3	Threshold of the daily average for hourly values
NO_2	10.5 ppb	60 ppb	Threshold of the daily average for hourly values
SO_2	1.9 ppb	40 ppb	Threshold of the daily average for hourly values

the amount of air pollutant is equal to the numerical criteria and a negative value indicating that the amount of air pollutant is larger than the numerical criteria.

The CII can be optimized according to users' requirements by selecting the air pollutants and setting the s values. The air pollutants we selected in the CII in this study were O_3, PM, NO_2 and SO_2 following the WHO AQG (WHO, 2005), i.e., N = 4. We set the values of s according to the Japanese Environmental Quality Standards (JEQS), which are given by the Ministry of the Environment (MOE) of Japan (Table 1). These air pollutants have been of importance for the last 5 decades in Japan, and have been monitored by AEROS from 1970. Surface O_3, which is harmful to human health (e.g., Liu et al., 2013) and crop yields and quality (e.g., Feng et al., 2015; Miao et al., 2017), has been increasing in Japan since the 1980s in spite of the decreasing O_3 precursors, such as NO_X and volatile organic compounds (VOCs) (Akimoto et al., 2015). Nagashima et al. (2017) estimated that the source of surface O_3 is increasing, and approximately 50 % of the total increase was caused by transboundary pollution from China and Korea. We used the criterion for photochemical oxidants (Ox) in the JEQS as the s value for O_3, because more than 90–95 % of Ox is composed of O_3. We used the suspended particulate matter (SPM) for PM following the JEQS, not $PM_{2.5}$, PM with a diameter of less than 2.5 μm, because the purpose of the CII is to estimate the level of air cleanness that is not a health risk. The amount of SPM was simply assumed as $[SPM] = ([PM_{10}] + [PM_{2.5}])/2$ in this study. NO_2 is a precursor of surface O_3 and is a harmful pollutant. It mostly originates from anthropogenic sources, especially fossil fuel combustion (e.g., power plants and vehicles). Major sources of SO_2 are emissions from volcanic eruptions (e.g., Read et al., 1993), as SO_2 emissions from anthropogenic sources have been reduced via regulatory policies (Wakamatsu et al., 2013).

3 Model simulation

A model simulation was performed to calculate the amounts of O_3, SPM, NO_2 and SO_2 of all Japanese municipalities (1896 in total; note that wards in megacities, such as Tokyo, Osaka, and Fukuoka were counted as independent municipalities), including municipalities with no stations to monitor air pollutants. We combined two regional models; The Weather Research and

https://doi.org/10.5194/gc-2019-16
Preprint. Discussion started: 6 September 2019

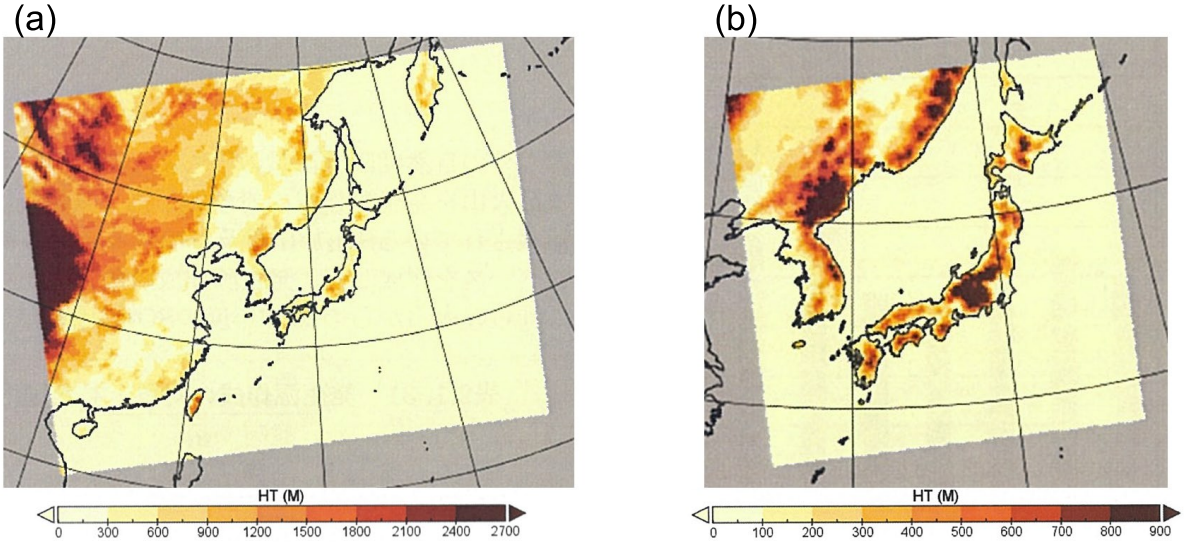

Figure 1. Ranges of (a) Domain 1 and (b) Domain 2 of the WRF-CMAQ models in this study. Color bars denote altitude.

Forecasting (WRF) model, for calculating meteorological fields (e.g., temperature, wind, and humidity), and the Community Multiscale Air Quality (CMAQ) model, calculating air pollutant amounts using the WRF results as input parameters. The calculations were made from 22 March 2014 to 31 March 2017, and the outputs from 1 April 2014 to 31 March 2017 were used for analyses. We selected the simulation period with a unit of fiscal year (FY), starting on 1 April and ending on 31 March, because the AEROS measurement dataset that we used to evaluate our simulation (Sect. 3.2) was archived with a unit of FY. The settings of the WRF-CMAQ model used in this study are described below.

3.1 WRF-CMAQ settings

We used the WRF model version 3.7 (Skamarock et al., 2008) to calculate the meteorological fields. We set two model domains; which Domain 1 covered East Asia with a horizontal grid resolution of 40 km and 157×123 grid points, and Domain 2 covered main-land Japan with a horizontal grid resolution of 20 km and 123×123 grid points, see Figure 1. The vertical layers consisted of 29 levels from the surface to 100 hPa. The initial and boundary conditions were obtained from the National Center for Environmental Prediction (NCEP) Final Operational Global Analysis (FNL, ds083.2) data (six-hourly, 1° × 1° resolution) (NCEP FNL, 2000). In the model domain, three-dimensional grid nudging for horizontal wind, temperature, and water vapor mixing ratio as well as two-dimensional grid nudging for sea surface temperature were performed every six hours. Furthermore, we used the following parameterizations: the new Thompson scheme (Thompson et al., 2008) for microphysical parameterization, the Dudhia scheme (Dudhia, 1989) and Rapid Radiative Transfer Model (Mlawer et al., 1997) for short- and longwave radiation processes, the Mellor-Yamada-Janjić scheme (Janjić, 1994) for planetary boundary layer parameterization, and the Betts-Yamada-Janjić scheme (Janjić, 1994) for cumulus parameterization.

https://doi.org/10.5194/gc-2019-16
Preprint. Discussion started: 6 September 2019

GEOSCIENCE COMMUNICATION Discussions
Open Access
EGU

The CMAQ model version 5.1 was used as a chemical transport model in this study. Byun and Schere (2006) provided an overview of the CMAQ model, and the updates and scientific evaluations of CMAQ version 5.1 are provided by Appel et al. (2017). The 2005 Carbon Bond (CB05) chemical mechanism with toluene update and additional chlorine chemistry (CB05TUCL Whitten et al., 2010; Sarwar et al., 2012) was used for the gas-phase chemistry. The used CMAQ model had two model domains, whose regions were the same as those adopted in the WRF model, see Figure 1, and vertical coordinates of 22 layers; the thickness of the lowest layer was approximately 30 m. The initial and boundary conditions of air pollutants for Domain 1 were obtained from the Model for OZone And Related chemical Tracers (MOZART) version 4 (Emmons et al., 2010), and the boundary conditions for Domain 2 were the model outputs of Domain 1.

Anthropogenic emissions were defined using the MIX Asian emission inventory version 1.1 which included emissions by power, industry, residential, transportation and agriculture (Li et al., 2017). This inventory of SO_2, NO_X, PM, VOC, CO and NH_3 for 2015 were estimated by correcting the 2010 data (2008 for NH_3) and implemented into the CMAQ model. The corrections were made using the statistical secular changes in the annual total anthropogenic emissions of pollutants and CO_2, population, amount of used chemical fertilizer and NH_3 emission by farm animals for each country included in the model domains (Japan, China, South Korea, North Korea, Taiwan, Mongolia, Vietnam, and Far East Russia). Biogenic emissions of VOC were provided by the Model of Emissions of Gases and Aerosols from Nature (MEGAN) version 2.10 (Guenther et al., 2012) using the meteorological fields calculated by the WRF model for 2016. The implemented emission inventories did not include interannual changes. Volcanic emissions of SO_2 were ignored, even though there are many active volcanos in Japan, because volcanic activities are irregular and difficult to reproduce.

The amount of pollutants in each Japanese municipality were defined at the longitude/latitude of the municipal office, with the weighted average of the outputs at model grid points near the municipal office using the following equation:

$$\overline{A} = \frac{1}{A_w} \sum_{i=1}^{I} \frac{R^2 - d_i^2}{R^2 + d_i^2} A_i, \quad A_w = \sum_{i=1}^{I} \frac{R^2 - d_i^2}{R^2 + d_i^2}, \tag{2}$$

where $\overline{A}$ is the defined amount of a pollutant at the municipal office, I (=2 or 3 mostly) is the number of the model grid points of Domain 2 within $R = \sqrt{0.02}$ degrees of the terrestrial central angle (approximately 16 km) from the office, and A_i and d_i are the simulated amount of a pollutant and distance from the office, respectively, at each model grid point. Note that Okinawa Prefecture and Ogasawara-mura municipality in Tokyo Prefecture were outside Domain 2, and the amount of pollutants at the municipalities in them were thus defined using the model outputs of Domain 1 with $R = \sqrt{0.08}$ degrees (approximately 31 km) in Eq. (2).

3.2 Evaluation: Comparison with in situ measurements

The CII value derived from the amounts of O_3, SPM, NO_2, and SO_2 calculated by the WRF-CMAQ model was compared with that measured by AEROS. AEROS is operated by the MOE of Japan and has 1901 observation sites for monitoring air pollutants in FY2016. The AEROS data were obtained from the atmospheric environment database of the National Institute for Environmental Studies (*Kankyosuchi database (in Japanese)*). We selected six cities for the comparison, i.e., Akita, Tokyo,

https://doi.org/10.5194/gc-2019-16
Preprint. Discussion started: 6 September 2019

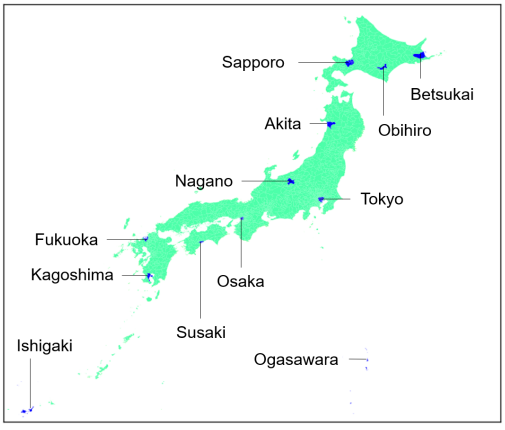

Figure 2. Location of Japanese municipalities focused on in this study.

Table 2. Correlation coefficient (r) of the CII, O_3, SPM, NO_2 and SO_2 between the WRF-CMAQ model simulation and the AEROS measurements in six Japanese cities. Numbers in parenthesis represent mean values of WRF-CMAQ (left) and AEROS (right) for the study period (FY2014–2016).

	Akita	Tokyo	Nagano	Osaka	Fukuoka	Kagoshima
CII	0.61 (0.80, 0.78)	0.68 (0.76, 0.75)	0.61 (0.78, 0.79)	0.73 (0.75, 0.71)	0.71 (0.75, 0.74)	0.65 (0.78, 0.77)
O_3 [ppb]	0.61 (33.4, 34.9)	0.67 (18.3, 26.9)	0.62 (40.0, 30.1)	0.71 (21.9, 28.0)	0.69 (26.1, 32.4)	0.62 (40.6, 27.1)
SPM [μg/m^3]	0.49 (12.0, 14.2)	0.53 (13.7, 19.3)	0.45 (10.7, 13.9)	0.57 (15.8, 21.5)	0.57 (20.9, 21.5)	0.31 (13.4, 22.0)
NO_2 [ppb]	0.25 (6.9, 6.9)	0.51 (25.3, 18.7)	0.15 (5.4, 9.1)	0.56 (23.5, 22.2)	0.37 (17.1, 13.7)	0.01 (2.2, 10.3)
SO_2 [ppb]	0.10 (1.1, 1.5)	0.36 (4.5, 2.2)	0.21 (1.0, 1.2)	0.52 (3.7, 4.2)	0.19 (3.1, 2.0)	−0.07 (0.9, 2.5)

Nagano, Osaka, Fukuoka and Kagoshima. The locations of these cities are shown in Fig. 2. Akita, Tokyo, Osaka, and Fukuoka were selected as representative cities of the four seasonal variation patterns of the surface O_3 in Japan: increase in spring in northeastern area (Akita), increase in spring and summer in Kanto area (Tokyo), increase in spring, summer, and autumn in Kansai area (Osaka), and increase in spring and autumn in western area (Fukuoka) (Akimoto et al., 2015). Nagano was selected as a rural area far from large anthropogenic emission sources. Kagoshima was selected to evaluate the effect of volcanic emission because there is active volcano in Sakurajima island, located approximately 5 km from the Kagoshima municipal office. The WRF-CMAQ results were averaged for all the wards in the comparison of Tokyo, Osaka and Fukuoka cities. The AEROS measurement results were averaged for all observation sites in each city, but in Tokyo, the observation sites in remote islands were omitted. The observation sites in Sakurajima island in Kagoshima were omitted because we ignored SO_2 emission from volcanic eruptions in our model as described in Sect. 3.1. In this comparison, the AEROS Ox data were compared to the WRF-CMAQ O_3 data because the composition ratio was larger than 90–95 % O_3 in Ox.

https://doi.org/10.5194/gc-2019-16
Preprint. Discussion started: 6 September 2019

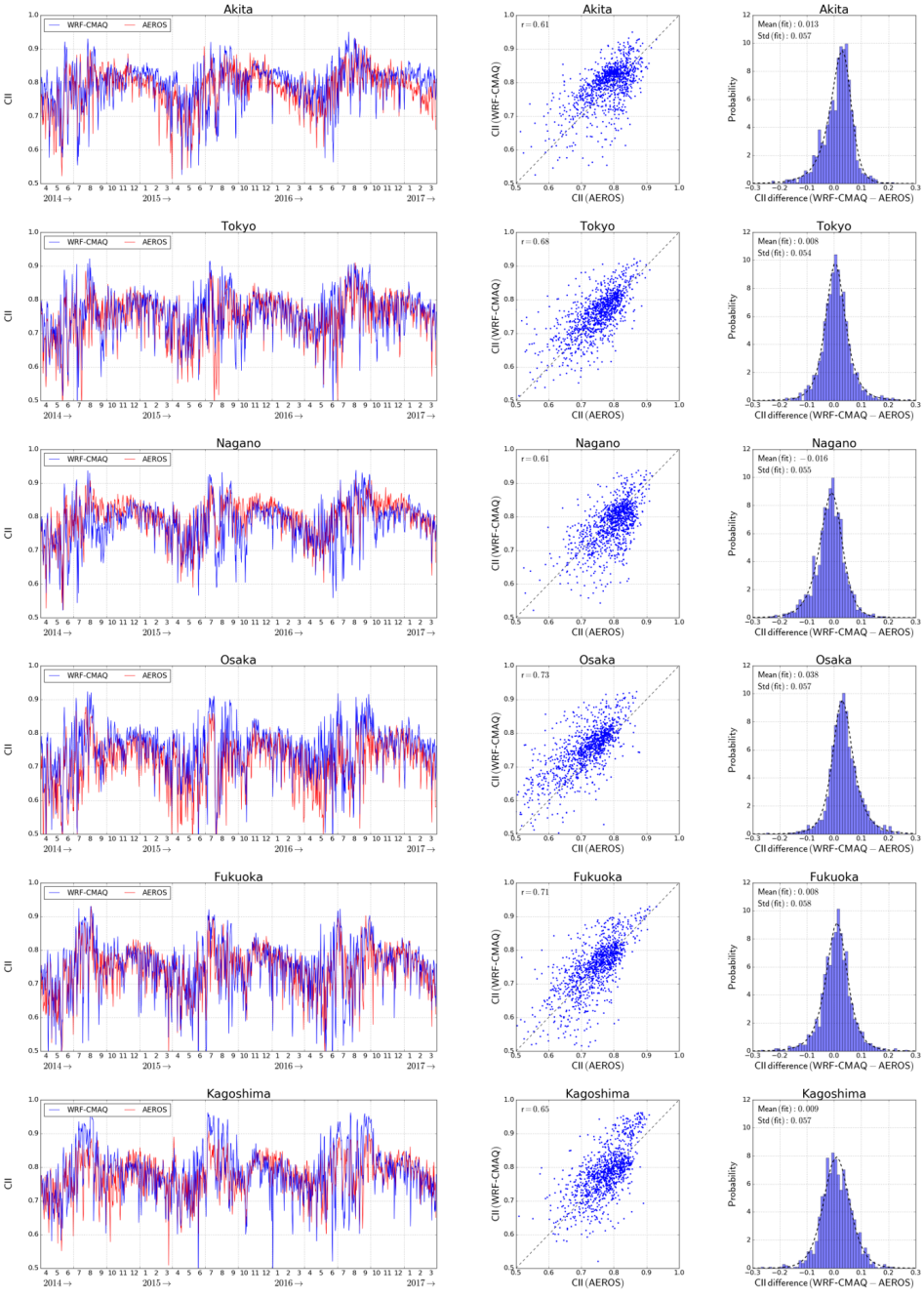

Figure 3. Comparison of CII derived from the WRF-CMAQ model and the AEROS measurements. Left column shows time variation of CII daily mean. Center column shows scatter plot of them with correlation coefficient (r). Right column shows histogram of differences in CII (WRF-CMAQ − AEROS). Dashed line is fitting curve with the Johnson SU function.

https://doi.org/10.5194/gc-2019-16
Preprint. Discussion started: 6 September 2019

GEOSCIENCE COMMUNICATION Discussions
Open Access
EGU

Time series variations in the daily CII mean derived from WRF-CMAQ and AEROS are compared in Fig. 3 (a). WRF-CMAQ and AEROS showed similar seasonal variations in the CII, i.e., increasing in spring to summer (May–August) and decreasing in autumn to winter (September–April). This seasonal variation in the CII was observed in the abovementioned six cities. The CII showed good agreement between WRF-CMAQ and AEROS with a correlation coefficient (r) of larger than 0.61. Table 2 shows the r values of the CII, O_3, SPM, NO_2, and SO_2 between WRF-CMAQ and AEROS for the six cities. The r values of the CII were higher than those of O_3, SPM, NO_2 and SO_2 in the 5 cities (not in Nagano), because the amounts of the species were normalized and comprehensively merged in the definition of CII in Eq. (1). This definition of CII relatively cancels discrepancies in each species in case that the amounts reciprocally vary as O_3 and NO_2 as below. NO_2 is a major precursor of O_3, and photolysis of NO_2 provides the oxygen atoms required to generate O_3 in the following reactions:

$$NO_2 + h\nu \rightarrow NO + O, \quad \text{(R1)}$$

$$O + O_2 + M \rightarrow O_3 + M, \quad \text{(R2)}$$

$$NO + O_3 \rightarrow NO_2 + O_2, \quad \text{(R3)}$$

where M is a third body for the ozone formation reaction. The model underestimates the amount of O_3 and overestimates that of NO_2 in case of large contribution of the reaction (R3), i.e., NO titration effect. This case was observed in the comparison in Tokyo, Osaka and Fukuoka, and the r values for CII were higher than those for O_3, and NO_2, see Table 2. Therefore, the cancellation of discrepancy in individual species in the definition of CII is a significant advantage for quantifying air cleanness using the proposed model.

We investigated the precision of the difference in the CII between the WRF-CMAQ model and AEROS measurements to clarify magnitude of significant differences in the CII derived from the WRF-CMAQ model. The histogram of the difference in the CII (WRF-CMAQ − AEROS), the right column of Fig. 3, shows an asymmetric distribution. We fitted the histogram by using the Johnson SU function, which is a probability distribution transformed from the Normal distribution to cover the asymmetry of the sample distribution (Johnson, 1949). The standard deviation (1-σ) of the fitted Johnson SU distribution was approximately 0.06 (0.054–0.067). It showed that the WRF-CMAQ model reproduced the CII value within a difference from AEROS of approximately 0.01 by averaging 30 values ($0.06/\sqrt{30} \approx 0.01$). Consequently, the difference in CII derived from the WRF-CMAQ larger than 0.01 was significant to be reproduced by AEROS by averaging 30 values.

4 Visualization of air cleanness in Japan

In Sect. 4, we discuss the area and season of high air cleanness in Japan. Figure 4 shows the average CII over the study period (FY2014–2016) for each Japanese municipality. The average CII and standard deviation (1-σ) of Tokyo was 0.75±0.07, which was 1.2 and 1.9 times higher than those of Seoul (0.64±0.13) and Beijing (0.39±0.29), respectively. The average CII of 89 % of municipalities were higher than that of Tokyo, and those of all the municipalities were higher than those of Seoul and Beijing.

https://doi.org/10.5194/gc-2019-16
Preprint. Discussion started: 6 September 2019

GEOSCIENCE COMMUNICATION
Discussions
Open Access
EGU

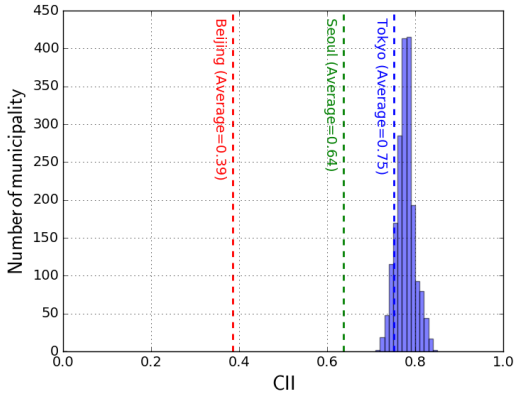

Figure 4. Histogram of average CII over the study period (FY2014–2016) for each municipality in Japan. Red, green, and blue dashed lines represent average CII of Beijing, Seoul, and Tokyo (23 wards), respectively.

4.1 Spatial-seasonal variation

The spatial-seasonal variations in CII, O_3, SPM, NO_2, and SO_2 in Japan are described in Sect. 4.1. Figure 5 (a) shows the daily mean CII value derived from the WRF-CMAQ model for each municipality over the study period. The horizontal and vertical axes correspond to the day and municipal number, respectively, and the lower municipal number corresponds approximately to the municipalities in northeast Japan and vice versa. This figure shows that the CII value depended on both area and season. The CII value tended to be higher in summer because of transportation of unpolluted air mass from the Pacific Ocean. In August 2014, July 2015 and September 2016, the CII values of almost all municipalities were higher than 0.9 for a few weeks. However, the local CII values decreased to below 0.55 over a short period because of local air pollutant emissions and the enhancement due to photochemical reactions induced by strong UV sunlight. The CII value was moderate (0.70–0.85) and stable from November to February over Japan but gradually decreased from February to May or June because polluted air was transported from East Asia, and the sunlight strengthened. The municipalities in Okinawa Prefecture, southernmost Japan, maintained their higher CII values of > 0.9 during this period.

The CII value depends not only on the amount of O_3, SPM, NO_2, and SO_2 (x), but also on their numerical criteria (s), see Eq. (1). A partial differentiation analysis was performed to determine the sensitivities of the s of O_3, SPM, NO_2, and SO_2 to CII. Figure 5 (b–e) shows the weighting function for the numerical criteria (K_s) given by

$$K_s[i] = \frac{\partial f(x,s)}{\partial s[i]} = \frac{1}{N}\frac{x[i]}{s[i]^2}. \quad (3)$$

In the definition of CII, Eq. (1), K_s positively correlates with x, and the CII value monotonically increases with increasing s. The seasonal variation in CII primarily corresponded with the variation in O_3. The average K_s for O_3 was highest among the species used to calculate the CII in this study, because the amount of O_3 was relatively higher than the value of s compared with SPM, NO_2, and SO_2 (Table 1). The value of K_s for SPM in western Japan was higher than that in eastern Japan during winter

https://doi.org/10.5194/gc-2019-16
Preprint. Discussion started: 6 September 2019

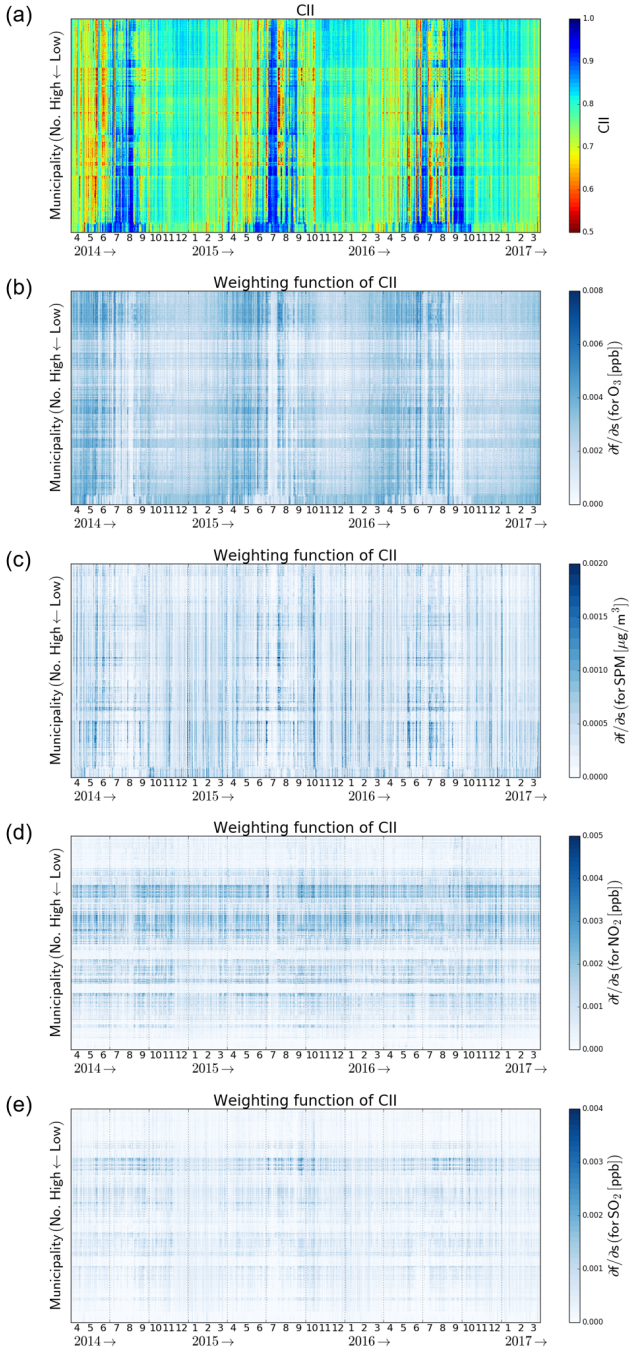

Figure 5. Spatial-seasonal variation in (a) CII and the weighting function for the numerical criteria, K_s, of (b) O_3, (c) SPM, (d) NO_2 and (e) SO_2 derived from the WRF-CMAQ model. The color scaling of (b–e) is optimized for each panel.

https://doi.org/10.5194/gc-2019-16
Preprint. Discussion started: 6 September 2019

GEOSCIENCE COMMUNICATION Discussions
Open Access
EGU

and spring because of the effect of transboundary pollution from East Asia. The spatial distribution of CII corresponded to those of K_s for NO_2 and SO_2, which explicitly reflected local emission sources, such as megacities and industrial areas. Typical lifetime of NO_2 is approximately a few hours, and the transport effect was therefore less for this species. We ignored SO_2 emissions from volcanic eruptions, and the SO_2 distribution consequently corresponded to industrial activities. No significant seasonal variation in K_s was observed for NO_2 and SO_2. The spatial distribution of O_3 was negatively correlated to that of NO_2 primarily because of the NO titration effect, reaction (R.3).

Consequently, the CII distribution was influenced not only by local emissions but also by transboundary pollution. The variation in O_3 had the most significant effect on seasonal variation in the CII. The spatial distribution of CII corresponded to those of NO_2 and SO_2. The SPM sources constituted both local emissions and transport from outside of Japan, and SPM variation affected both spatial and seasonal variations in CII.

4.2 Area and season of high air cleanness

In Sect. 4.2, we discuss the area and season of highest air cleanness over Japan using the CII. First, the CII average over the study period, FY2014–2016, in each municipality was compared, Fig. 6 (a), and the daily mean value for this period was averaged for each municipality. The CII averages in northern Japan were higher, and those in municipalities around megacities and industrial areas were lower than the average of all municipalities, 0.78 ± 0.05 (1-σ). Table 3 shows the 10 municipalities with the highest average CII values, which all located in eastern Hokkaido. The average CII was approximately 0.83–0.84 in these 10 municipalities, and the standard deviation (1-σ) over the study period was lower than that in other areas, see Fig. 6 (b). The CII remained high throughout the year. For example, the CII daily mean in Betsukai-cho municipality, where the three-year CII average was the highest, was higher than the total municipal average of 0.78 in 91 % of days over the study period.

We discuss the CII distribution in case of high CII average of all Japanese municipalities. We selected 10 days per year, a total of 30 days, with the highest average CII values to discuss the CII distribution by same-order precision of 0.01 with the AEROS measurements, see Sect. 3.2 (7/9, 7/10, 8/9, 8/10, 8/15–8/20 in 2014; 7/13–7/19, 7/22, 8/17, 9/10 in 2015; and 7/9, 8/21, 9/7, 9/12–9/14, 9/19, 9/25, 9/27, 9/28 in 2016). These 30 days were selected in summer when unpolluted air was transported from the Pacific Ocean. The average CII values on these 30 days for each municipality are displayed in Fig. 6 (c), and Table 4 shows the 10 municipalities with the highest average CII values on these days. These 10 municipalities located around western Pacific coast, i.e., Kochi, Mie and Wakayama Prefectures, and southern remote islands of Tokyo. The average CII of Susaki-shi municipality in Kochi Prefecture was the highest. The average CII of these 10 municipalities was approximately 0.93, which was 1.1 times higher than that of all Japanese municipalities on high-CII days (0.88). Therefore, the highest CII value occurred on the Pacific coast during summer with the condition of few local pollution.

Similar to the high-CII case, 30 days with the lowest CII average of all Japanese municipalities were selected (4/25, 4/26, 5/13, 5/29–6/2, 6/16, 7/12 in 2014; 4/16, 4/24, 4/26, 4/27, 5/13, 5/22, 5/27, 6/12, 6/13, 7/31 in 2015; and 5/4, 5/27, 5/28, 5/31, 6/17, 6/18, 6/25, 6/26, 8/31, 9/1 in 2016). The average of CII values on these 30 low-CII days for each municipality are displayed in Fig. 6 (d), and Table 5 shows the 10 municipalities with the highest average CII values on these days. These 10 municipalities located in remote islands, such as Ogasawara-mura in Tokyo and Ishigaki-chi in Okinawa. The average CII in

https://doi.org/10.5194/gc-2019-16
Preprint. Discussion started: 6 September 2019

Geoscience Communication Discussions
Open Access
EGU

Table 3. Ten municipalities with highest average CII value over the study period, FY2014–2016. The municipal number is shown in parenthesis.

Municipality	Prefecture	CII
Betsukai-cho (1691)	Hokkaido	0.840
Hamanaka-cho (1663)	Hokkaido	0.840
Shibecha-cho (1664)	Hokkaido	0.839
Akkeshi-cho (1662)	Hokkaido	0.838
Nakashibetsu-cho (1692)	Hokkaido	0.838
Shiranuka-cho (1668)	Hokkaido	0.837
Tsurui-mura (1667)	Hokkaido	0.835
Nemuro-shi (1223)	Hokkaido	0.834
Shibetsu-cho (1693)	Hokkaido	0.832
Saroma-cho (1552)	Hokkaido	0.832
Average of all Japanese municipalites		0.778

Table 4. Same as Table 3 but for the average CII for the 30 high-CII days.

Municipality	Prefecture	CII
Susaki-shi (39206)	Kochi	0.934
Tsuno-cho (39411)	Kochi	0.933
Hachijo-machi (13401)	Tokyo	0.933
Kumano-shi (24212)	Mie	0.933
Kitayama-mura (30427)	Wakayama	0.933
Mikurajima-mura (13382)	Tokyo	0.933
Nakatosa-cho (39401)	Kochi	0.933
Aogashima-mura (13402)	Tokyo	0.932
Sakawa-cho (39402)	Kochi	0.932
Miyake-mura (13381)	Tokyo	0.931
Average of all Japanese municipalites		0.880

https://doi.org/10.5194/gc-2019-16
Preprint. Discussion started: 6 September 2019

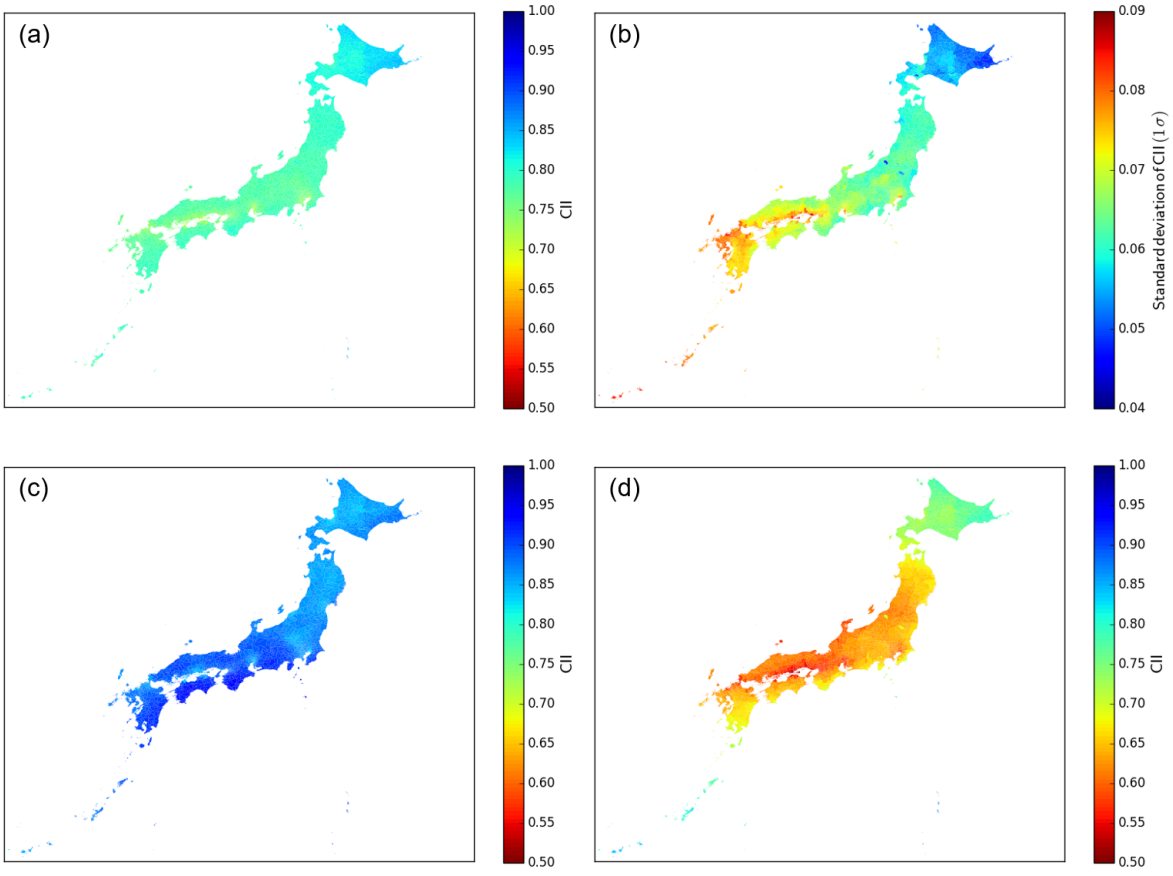

Figure 6. Spatial distributions of CII derived from the WRF-CMAQ model. (a) Mean over the study period (FY2014–2016). (b) Same as (a) but for standard deviation (1-σ). (c) Mean for 30 days of highest CII average in all Japanese municipalities (10 days from each FY). (d) Same as (c) but for lowest CII average.

these municipalities was 0.82–0.85, which was approximately 1.3 times larger than that of all municipalities on low-CII days (0.64). The selected 30 days occurred especially at the end of spring and beginning of summer. Generally, the transboundary pollution effect is large in spring, and heavy local pollution occurs in summer because of photochemical reactions induced by strong sunlight. These pollution effects are less pronounced in the remote islands, thus the CII maintained higher values.

225 We selected "Top 100 clean air cities" in Japan using the CII. The 30 highest daily mean CII values in the study period were averaged for each municipality. Table 6 shows the 100 municipalities with the highest average CII values. The municipalities in remote islands of Tokyo, and around western Japan, especially around the Pacific coast, i.e., Wakayama, Tokushima, Ehime, Kochi, Kumamoto, Oita, Miyazaki, Kagoshima and Okinawa Prefectures, were selected.

https://doi.org/10.5194/gc-2019-16
Preprint. Discussion started: 6 September 2019

Table 5. Same as Table 3 but for the average CII for the 30 low-CII days.

Municipality	Prefecture	CII
Ogasawara-mura (13421)	Tokyo	0.852
Ishigaki-shi (47207)	Okinawa	0.840
Taketomi-cho (47381)	Okinawa	0.840
Miyakojima-shi (47214)	Okinawa	0.835
Tarama-son (47375)	Okinawa	0.835
Minamidaito-son (47357)	Okinawa	0.832
Yonaguni-cho (47382)	Okinawa	0.829
Kitadaito-son (47358)	Okinawa	0.828
Kunigami-son (47301)	Okinawa	0.824
Higashi-son (47303)	Okinawa	0.824
Average of all Japanese municipalites		0.644

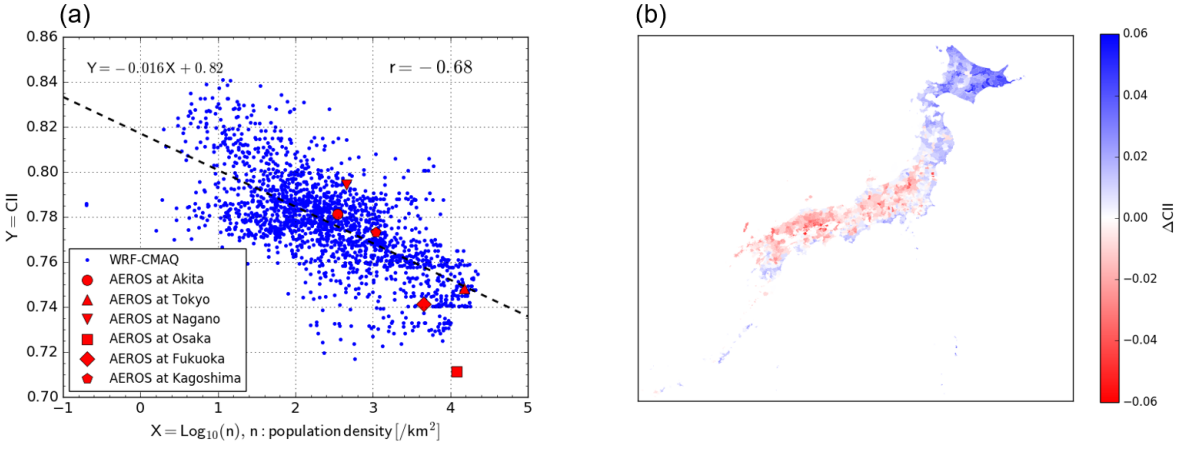

Figure 7. (a) Comparison of CII and population density (n) in each Japanese municipality. Blue dot shows the WRF-CMAQ results. Black dashed line shows linear regression of CII with $\log_{10}(n)$. Correlation coefficient (r) between CII values and $\log_{10}(n)$ is shown in the upper right side. Red markers show the CII derived from the AEROS measurements in six cities (Akita, Tokyo, Nagano, Osaka, Fukuoka, and Kagoshima). (b) Distribution of differences in CII from the linear regression (ΔCII).

4.3 Air cleanness and human activities

Industrial activities, particularly fossil fuel combustion such as vehicles and power plants, are major sources of air pollutants, and air cleanness is strongly related with human activities. It is generally difficult to maintain clean air with large-scale indus-

https://doi.org/10.5194/gc-2019-16
Preprint. Discussion started: 6 September 2019

Geoscience Communication Discussions
Open Access
EGU

Table 6. "Top 100 clean air cities" in Japan. The municipal number is shown in parenthesis.

Municipality	Prefecture
Niijima-mura (13363), Kozushima-mura (13364), Miyake-mura (13381), Mikurajima-mura (13382)	Tokyo
Hachijo-machi (13401), Aogashima-mura (13402), Ogasawara-mura (13421)	
Tanabe-shi (30206), Minabe-cho (30391), Shirahama-cho (30401), Kamitonda-cho (30404)	Wakayama
Nachikatsuura-cho (30421), Kozagawa-cho (30424), Kushimoto-cho (30428)	
Kaiyo-cho (36388)	Tokushima
Uwajima-shi (38203), Seiyo-shi (38214), Matsuno-cho (38484), Kihoku-cho (38488)	Ehime
Ainan-cho (38506)	
Kochi-shi (39201), Aki-shi (39203), Nankoku-shi (39204), Tosa-shi (39205)	Kochi
Susaki-shi (39206), Sukumo-shi (39208), Tosashimizu-shi (39209), Shimanto-shi (39210)	
Konan-shi (39211), Kami-shi (39212), Toyo-cho (39301), Nahari-cho (39302)	
Tano-cho (39303), Yasuda-cho (39304), Kitagawa-mura (39305), Umaji-mura (39306)	
Geisei-mura (39307), Ino-cho (39386), Niyodogawa-cho (39387), Nakatosa-cho (39401)	
Sakawa-cho (39402), Ochi-cho (39403), Yusuhara-cho (39405), Hidaka-mura (39410)	
Tsuno-cho (39411), Shimanto-cho (39412), Otsuki-cho (39424), Mihara-mura (39427)	
Kuroshio-cho (39428)	
Taragi-machi (43505), Yunomae-machi (43506), Mizukami-mura (43507), Asagiri-cho (43514)	Kumamoto
Saiki-shi (44205)	Oita
Miyazaki-shi (45201), Miyakonojyo-shi (45202), Nobeoka-shi (45203), Nichinan-shi (45204)	Miyazaki
Kobayashi-shi (45205), Hyuga-shi (45206), Kushima-shi (45207), Saito-shi (45208)	
Ebino-shi (45209), Mimata-cho (45341), Takaharu-cho (45361), Kunitomi-cho (45382)	
Aya-cho (45383), Takanabe-cho (45401), Shintomi-cho (45402), Nishimera-son (45403)	
Kijyo-cho (45404), Kawaminami-cho (45405), Tsuno-cho (45406), Kadogawa-cho (45421)	
Morotsuka-son (45429), Shiiba-son (45430), Misato-cho (45431), Takachiho-cho (45441)	
Hinokage-cho (45442), Gokase-cho (45443)	
Kanoya-shi (46203), Makurazaki-shi (46204), Ibusuki-shi (46210), Nishinoomote-shi (46213)	Kagoshima
Soo-shi (46217), Kirishima-shi (46218), Shibushi-shi (46221), Amami-shi (46222)	
Minamikyushu-shi (46223), Yusui-cho (46452), Osaki-cho (46468), Higashikushira-cho (46482)	
Kinko-cho (46490), Minamiosumi-cho (46491), Kimotsuki-cho (46492), Nakatane-cho (46501)	
Minamitane-cho (46502), Yakushima-cho (46505), Yamato-son (46523)	
Minamidaito-son (47357), Kitadaito-son (47358)	Okinawa

https://doi.org/10.5194/gc-2019-16
Preprint. Discussion started: 6 September 2019

Geoscience Communication Discussions
Open Access
EGU

Table 7. Ten municipalities with highest average ΔCII value over the study period, FY2014–2016. The municipal number is shown in parenthesis.

Municipality	Prefecture	ΔCII	CII
Obihiro-shi (1207)	Hokkaido	0.050	0.827
Sapporo-shi, Atsubetsu-ku (1108)	Hokkaido	0.049	0.805
Kushiro-shi (1206)	Hokkaido	0.048	0.830
Sapporo-shi, Shiroishi-ku (1104)	Hokkaido	0.046	0.802
Nemuro-shi (1223)	Hokkaido	0.046	0.834
Nakashibetsu-cho (1692)	Hokkaido	0.046	0.838
Kushiro-cho (1661)	Hokkaido	0.045	0.831
Sapporo-shi, Chuo-ku (1101)	Hokkaido	0.043	0.800
Sapporo-shi, Toyohira-ku (1105)	Hokkaido	0.043	0.800
Sapporo-shi, Higashi-ku (1103)	Hokkaido	0.043	0.800
Average of all Japanese municipalites		−0.000	0.778

trial activities, and it is therefore not fair to directly compare air cleanness in municipalities with different human activities. In Sect. 4.3, we discuss the relationship between air cleanness, i.e., CII, and the scale of human activities.

In this study, the common logarithm of population density (n), $\log_{10}(n)$, was employed to quantify human activities (e.g., Kerr and Currie, 1995). The n data were obtained from the 2015 Japanese national census (NSTAC, 2016). Figure 7 (a) shows the scatter plot of $\log_{10}(n)$ and average CII for the study period, FY2014–2016, derived from the WRF-CMAQ model for each municipality. A clear negative correlation between $\log_{10}(n)$ and the CII was observed and had an r value of -0.68. This negative correlation was formulated by the linear regression with the objective variable of CII and the explanatory variable of $\log_{10}(n)$, as shown by the black dashed line in Fig. 7 (a).

$$\mathrm{CII} = -0.016 \times \log_{10}(n) + 0.82 \tag{4}$$

The red markers indicate the CII values derived from the AEROS measurements at the six cities used for comparison study (Fig. 3). The negative correlation between the CII value and $\log_{10}(n)$ was reproduced from the AEROS measurements and agreed with the linear regression line, except for Osaka.

The linear regression line, Eq. (4), normalized the CII values by the population density n. The difference between the CII and the linear regression line (ΔCII) can be an additional indicator compensating for the unfair comparison of air cleanness caused by human activities. The distribution of ΔCII in the average for FY2014–2016 is shown in Fig. 7 (b), and Table 7 shows the 10 municipalities with the highest average ΔCII values. All of these municipalities were in Hokkaido, similar to the results shown in Table 3, but urban municipalities in Hokkaido were ranked as Sapporo-shi and Obihiro-shi cities. The ΔCII values in northeastern Japan, especially Hokkaido, were higher than those in western Japan. The ΔCII value reflects the transport of

https://doi.org/10.5194/gc-2019-16
Preprint. Discussion started: 6 September 2019

GEOSCIENCE COMMUNICATION Discussions
Open Access
EGU

air pollutants from around the municipality rather than the CII value if the neighboring municipality was a megacity or had industrial factories. There are many industrial areas in western Japan, which might be one reason for the lower ΔCII values. As discussed above, ΔCII quantified the air cleanness with respect to population density, i.e., human activities. The combination of CII and ΔCII could be a useful way of evaluating air cleanness.

5 Conclusions

We defined a novel concept of index for quantifying air cleanness, namely CII. This index comprehensively evaluates the level of air cleanness by normalizing the amounts of common air pollutants. A CII value of 1 indicates the absence of air pollutants, and 0 indicates that the amounts of air pollutants are the same as the normalization numerical criteria.

A model simulation was performed to visualize the air cleanness of all 1896 municipalities in Japan using CII. We used O_3, SPM, NO_2, and SO_2 in CII, and their numerical environmental criteria were taken from the JEQS set by the MOE of Japan. The amounts of these species were calculated via the model combining the WRF model version 3.7 and CMAQ model version 5.1. The time period of the simulation was from 1 April 2014 to 31 March 2017, i.e., FY2014–2016. The CII value near the surface derived from the model was evaluated by comparing it with AEROS in situ observations, operated by the MOE of Japan, in Akita, Tokyo, Nagano, Osaka, Fukuoka, and Kagoshima, which cover areas of four patterns of O_3 seasonal variation, a rural area and an area affected by volcanic eruption. The CII correlation coefficient r between the WRF-CMAQ and AEROS exceeded 0.61.The precision of the difference in CII between the WRF-CMAQ and AEROS was approximated by the Johnson SU function. The CII difference derived from the WRF-CMAQ larger than 0.01 was significant and could be reproduced by AEROS by averaging 30 values.

Over the study period, FY2014–2016, eastern Hokkaido had the highest CII average values of 0.83–0.84, which were 1.1 times higher than the average values of all Japanese municipalities of 0.78. The average CII value of Tokyo (23 wards) was 0.75, which was 1.2 and 1.9 times higher than those of Seoul (0.64) and Beijing (0.39), respectively. The CII value varied spatially and temporally, corresponding to variations in O_3, SPM, NO_2, and SO_2. The extremely clean air with CII values around 0.93, occurred around western the Pacific coast, i.e., Kochi, Mie and Wakayama Prefectures, and southern remote islands of Tokyo during summer with transport of unpolluted air from the ocean. The municipalities in remote islands, such as Ogasawara and Okinawa maintained their high CII values of 0.82–0.85, which was approximately 1.3 times higher than the average of all municipalities. Furthermore, "Top 100 clean air cities" in Japan was presented using the CII.

The relationship between air cleanness and human industrial activities could not be fairly compared. Population density was used to quantify human activities in this study. The CII (Y) was approximated by a linear function of the common logarithm of population density (X), $Y = -0.016X + 0.82$. The differences in CII from this approximation line (ΔCII) in northeastern Japan, especially Hokkaido, were higher than those in western Japan. The east-west contrast of ΔCII might be due to large-scale industrial activities in western Japan. A combination of CII and ΔCII could be a useful way of evaluating air cleanness.

The CII can be used in various scenarios, such as encouraging sightseeing and migration, insurance company business, and city planning. For example, Hokkaido is recommended to live because the CII value is constantly high throughout the year.

https://doi.org/10.5194/gc-2019-16
Preprint. Discussion started: 6 September 2019

Western the Pacific coast and southern remote islands can be tourist spots for seeking "tasty air" because extremely high CII values are temporally given during summer. The CII enabled the quantitative evaluation of air cleanness, and could not only be applied in Japan but also in other countries.

Data availability. The WRF-CMAQ model data in this publication can be accessed by contacting the authors. The AEROS measurement data are available through the following link: https://www.nies.go.jp/igreen. Japanese population density data are available through the following link: https://www.e-stat.go.jp/.

Video supplement. The CII daily mean for all 1896 Japanese municipalities is archived for each month over the study period, FY2014–2016.

Author contributions. Conceptualization, All authors; Model simulation, T. K.; Evaluation of data quality; T. O. S.; Manuscript writing, T. O. S. and T. K.; Writing significant contribution to paper, Y. K.; Review and editing, All authors.

Competing interests. The authors declare that they have no conflict of interest.

Acknowledgements. The WRF-CMAQ model simulation was performed by the computing system in the NICT Science cloud. We would like to thank the Big Data Analytics Laboratory of NICT and Suuri-Keikaku Co., Ltd. for supporting the computation. We gratefully acknowledge Iwao Hosako and Motoaki Yasui for their kind management of the research environment in NICT. We deeply appreciate Hideyuki Teraoka in Ministry of Internal Affairs and Communications to give us an idea "TOP 100 clean air cities". TOS thanks to Seidai Nara for his polite technical support.

https://doi.org/10.5194/gc-2019-16
Preprint. Discussion started: 6 September 2019

Geoscience Communication Discussions
Open Access
EGU

References

Akimoto, H., Mori, Y., Sasaki, K., Nakanishi, H., Ohizumi, T., and Itano, Y.: Analysis of monitoring data of ground-level ozone in Japan for long-term trend during 1990–2010: Causes of temporal and spatial variation, Atmos. Env., 102, 302–310, https://doi.org/10.1016/j.atmosenv.2014.12.001, 2015.

Appel, K. W., Napelenok, S. L., Foley, K. M., Pye, H. O. T., Hogrefe, C., Luecken, D. J., Bash, J. O., Roselle, S. J., Pleim, J. E., Foroutan, H., Hutzell, W. T., Pouliot, G. A., Sarwar, G., Fahey, K. M., Gantt, B., Gilliam, R. C., Heath, N. K., Kang, D., Mathur, R., Schwede, D. B., Spero, T. L., Wong, D. C., and Young, J. O.: Description and evaluation of the Community Multiscale Air Quality (CMAQ) modeling system version 5.1, Geoscientific Model Development, 10, 1703–1732, https://doi.org/10.5194/gmd-10-1703-2017, 2017.

Byun, D. and Schere, K. L.: Review of the Governing Equations, Computational Algorithms, and Other Components of the Models-3 Community Multiscale Air Quality (CMAQ) Modeling System, Applied Mechanics Reviews, 59, 51, https://doi.org/10.1115/1.2128636, 2006.

Dudhia, J.: Numerical Study of Convection Observed during the Winter Monsoon Experiment Using a Mesoscale Two-Dimensional Model., J. Atmos. Sci., 46, 3077–3107, https://doi.org/10.1175/1520-0469(1989)046<3077:NSOCOD>2.0.CO;2, 1989.

Emmons, L. K., Walters, S., Hess, P. G., Lamarque, J. F., Pfister, G. G., Fillmore, D., Granier, C., Guenther, A., Kinnison, D., Laepple, T., Orlando, J., Tie, X., Tyndall, G., Wiedinmyer, C., Baughcum, S. L., and Kloster, S.: Description and evaluation of the Model for Ozone and Related chemical Tracers, version 4 (MOZART-4), Geoscientific Model Development, 3, 43–67, 2010.

Feng, Z., Hu, E., Wang, X., Jiang, L., and Liu, X.: Ground-level O_3 pollution and its impacts on food crops in China: a review, Environ. Pollut., 199, 42–48, https://doi.org/10.1016/j.envpol.2015.01.016, 2015.

Guenther, A. B., Jiang, X., Heald, C. L., Sakulyanontvittaya, T., Duhl, T., Emmons, L. K., and Wang, X.: The Model of Emissions of Gases and Aerosols from Nature version 2.1 (MEGAN2.1): an extended and updated framework for modeling biogenic emissions, Geoscientific Model Development, 5, 1471–1492, https://doi.org/10.5194/gmd-5-1471-2012, 2012.

Janjić, Z. I.: The Step-Mountain Eta Coordinate Model: Further Developments of the Convection, Viscous Sublayer, and Turbulence Closure Schemes, Monthly Weather Review, 122, 927, https://doi.org/10.1175/1520-0493(1994)122<0927:TSMECM>2.0.CO;2, 1994.

Johnson, N. L.: Systems of Frequency Curves Generated by Methods of Translation, Biometrika, 36, 149–176, https://doi.org/10.2307/2332539, 1949.

Kerr, J. T. and Currie, D. J.: Effects of human activity on global extinction risk, Conserv. Biol., 9, 1528–1538, 1995.

Li, M., Zhang, Q., Kurokawa, J.-i., Woo, J.-H., He, K., Lu, Z., Ohara, T., Song, Y., Streets, D. G., Carmichael, G. R., Cheng, Y., Hong, C., Huo, H., Jiang, X., Kang, S., Liu, F., Su, H., and Zheng, B.: MIX: a mosaic Asian anthropogenic emission inventory under the international collaboration framework of the MICS-Asia and HTAP, Atmos. Chem. Phys., 17, 935–963, https://doi.org/10.5194/acp-17-935-2017, 2017.

Liu, T., Li, T. T., Zhang, Y. H., Xu, Y. J., Lao, X. Q., Rutherford, S., Chu, C., Luo, Y., Zhu, Q., Xu, X. J., Xie, H. Y., Liu, Z. R., and Ma, W. J.: The short-term effect of ambient ozone on mortality is modified by temperature in Guangzhou, China, Atmos. Env., 76, 59–67, https://doi.org/10.1016/j.atmosenv.2012.07.011, 2013.

McCarty, J. and Kaza, N.: Urban form and air quality in the United States, Landscape and Urban Planning, 139, 168–179, https://doi.org/https://doi.org/10.1016/j.landurbplan.2015.03.008, 2015.

Miao, W., Huang, X., and Song, Y.: An economic assessment of the health effects and crop yield losses caused by air pollution in mainland China, J. Environ. Sci., 56, 102–113, https://doi.org/10.1016/j.jes.2016.08.024, 2017.

https://doi.org/10.5194/gc-2019-16
Preprint. Discussion started: 6 September 2019

Mlawer, E. J., Taubman, S. J., Brown, P. D., Iacono, M. J., and Clough, S. A.: Radiative transfer for inhomogeneous atmospheres: RRTM, a validated correlated-k model for the longwave, J. Geophys. Res., 102, 16 663–16 682, https://doi.org/10.1029/97JD00237, 1997.

Nagashima, T., Sudo, K., Akimoto, H., Kurokawa, J., and Ohara, T.: Long-term change in the source contribution to surface ozone over Japan, Atmos. Chem. Phys., 17, 8231–8246, https://doi.org/10.5194/acp-17-8231-2017, 2017.

NCEP FNL: National Centers for Environmental Prediction/National Weather Service/NOAA/U.S.Department of Commerce (2000), Updated Daily. NCEP FNL Operational Model Global Tropospheric Analyses, Continuing from July 1999, Research Data Archive at the National Center for Atmospheric Research. Computational and Information Systems Laboratory., https://doi.org/10.5065/D6M043C6, 2000.

NSTAC: Portal Site of Official Statistics of Japan website, 2015 Population Census, https://www.e-stat.go.jp/<lastaccesson15August2019>, 2016.

OECD: The Economic Consequences of Outdoor Air Pollution. Policy Highlights, OECD Publishing, 2016.

Read, W. G., Froidevaux, L., and Waters, J. W.: Microwave limb sounder measurement of stratospheric SO_2 from the Mt. Pinatubo Volcano, Geophys. Res. Lett., 20, 1299–1302, https://doi.org/10.1029/93GL00831, 1993.

Sarwar, G., Simon, H., Bhave, P., and Yarwood, G.: Examining the impact of heterogeneous nitryl chloride production on air quality across the United States, Atmos. Chem. Phys., 12, 6455–6473, https://doi.org/10.5194/acp-12-6455-2012, 2012.

Skamarock, W. C., Klemp, J. B., Dudhia, J., Gill, D. O., Barker, D. M., Duda, M. G., Huang, X. Y., Wang, W., and Powers, J. G.: A discription of the Advanced Research WRF Version 3, NCAR Technical Note NCAR/TN-475+STR, 2008.

Stieb, D. M., Burnett, R. T., Smith-Doiron, M., Brion, O., Shin, H. H., and Economou, V.: A New Multipollutant, No-Threshold Air Quality Health Index Based on Short-Term Associations Observed in Daily Time-Series Analyses, J. Air & Waste Manage. Assoc., 58, 435–450, https://doi.org/10.3155/1047-3289.58.3.435, 2008.

Thompson, G., Field, P. R., Rasmussen, R. M., and Hall, W. D.: Explicit Forecasts of Winter Precipitation Using an Improved Bulk Microphysics Scheme. Part II: Implementation of a New Snow Parameterization, Monthly Weather Review, 136, 5095, https://doi.org/10.1175/2008MWR2387.1, 2008.

US EPA: Guidelines for the Reporting of Daily Air Quality, the Air Quality Index (AQI), EPA-454/B-06-001, pp. 8–14, 2006.

Wakamatsu, S., Morikawa, T., and Ito, A.: Air pollution trends in Japan between 1970 and 2012 and impact of urban air pollution countermeasures, Asian Journal of Atmospheric Environment, 7, 177–190, 2013.

Whitten, G. Z., Heo, G., Kimura, Y., McDonald-Buller, E., Allen, D. T., Carter, W. P. L., and Yarwood, G.: A new condensed toluene mechanism for Carbon Bond: CB05-TU, Atmos. Env., 44, 5346–5355, https://doi.org/10.1016/j.atmosenv.2009.12.029, 2010.

WHO: WHO Air Quality Guidelines Global Update 2005, Report of a Working Group Meeting, Bonn, Germany, 2005.

Wong, T. W., Tama, W. W. S., Yu, I. T. S., Lau, A. K. H., Pang, S. W., and Wong, A. H.: Developing a risk-based air quality health index, Atmos. Env., 76, 52–58, https://doi.org/10.1016/j.atmosenv.2012.06.071, 2013.